Trimethylamine Induced Chronic Kidney Injury by Activating the ZBP1-NLRP3 Inflammasome Pathway

Lu BAI[1]*, Qian CHEN[1]*, Yanqing LI[2], Fen WU[3], Mingzhe JIN[2], Yuhong CHEN[4], Xu TENG[1], Sheng JIN[1], Huanfang FAN[2], Yuming WU[1,5]

** These authors contributed equally to this work.*

[1]Department of Physiology, Hebei Medical University, Hebei, China, [2]Hebei Provincial Hospital of Chinese Medicine, Hebei University of Chinese Medicine, Hebei, China, [3]Liaocheng Third People's Hospital, Shangdong, China, [4]The Fourth Hospital of Hebei Medical University, Hebei, China, [5]Hebei Collaborative Innovation Center for Cardio-Cerebrovascular Disease, Hebei, China

Received April 2, 2024
Accepted June 18, 2024

Summary

Trimethylamine N-oxide (TMAO), a bioactive metabolite of gut microbes, plays a pivotal role in the pathogenesis of kidney diseases by activating programmed cell death (PCD) pathways. However, whether trimethylamine (TMA) contributes to chronic kidney injury and which kind of PCD is involved in TMA-induced chronic kidney injury has not been previously evaluated. To observe the effect of TMA, male C57BL/6J mice were randomly divided into two groups: the Control group and the TMA group. The mice in the TMA group were intraperitoneally injected with 100 μmol/kg/day TMA for three months, whereas the mice in the Control group were injected with normal saline for the same period. After three months, plasma creatinine and blood urea nitrogen levels, indicators of kidney function, increased significantly in the TMA group as compared with those in the Control group. Furthermore, Masson staining assay showed that TMA treatment led to a larger area of fibrosis than the Control group. TMA treatment did not change the Bax/Bcl-2 ratio, RIP1, RIP3 and MLKL phosphorylation, or iron and malondialdehyde levels in kidney tissues, indicating that apoptosis, ferroptosis and necroptosis were not involved in TMA-induced chronic kidney injury. However, compared with the Control group, TMA treatment significantly upregulated NLRP3, Caspase-1, IL-1β, cleaved-Caspase 8, Caspase-8, and ZBP1 protein expression in kidney tissues. These results indicated that the ZBP1-NLRP3 inflammasome pathway was involved in TMA-induced chronic kidney injury. In conclusion, our studies revealed that the ZBP1-NLRP3 inflammasome may take part in the progression of TMA induced chronic kidney injury.

Key words

Trimethylamine • Chronic kidney injury • ZPB1 • NLRP3 inflammasome

Corresponding authors

Y. Wu, Department of Physiology, Hebei Medical University, 361 Zhongshan Road, Shijiazhuang 050017, China. E-mail: wuyum@yahoo.com and H. Fan, Hebei Provincial Hospital of Chinese Medicine, Hebei University of Chinese Medicine, 389 Zhongshan Road Shijiazhuang 050017, China. E-mail: fhf701024@163.com

Introduction

Chronic kidney disease (CKD) is a clinical syndrome secondary to various causative factors induced by kidney damage and is characterized by an irreversible and progressive loss of kidney functions. Currently, it is a major public health concern with an increased prevalence with age [1]. Therefore, it is crucial to elucidate the exact pathogenic mechanisms for effective management. Accumulating evidence has shown a strong association between gut microbe-derived metabolites and CKD onset and development [2]. Trimethylamine (TMA) is a gut microbiota-derived metabolite which comes from diets rich in choline, betaine or L-carnitine by intestinal microbial enzymes (such as CutC/D and CntA/B) and can be further converted to trimethylamine N-oxide (TMAO) in the liver by the host enzyme flavin-containing monooxygenase 3. As a bioactive metabolite of gut

microbes, TMAO plays a pivotal role in the pathogenesis of various diseases, including cardiovascular disease, neurological disorders, and most importantly, CKD development [3-4]. Some clinical studies have demonstrated that circulating TMAO levels was accumulated in CKD patients and increased with the severity of kidney function damage [5]. Some animal studies have suggested that chronic dietary exposure to either choline or TMAO can cause progressive renal fibrosis and dysfunction [6-7]. However, other studies have found that TMAO had a beneficial effect [8], whereas TMA but not TMAO had a negative effect [9]. Therefore, it is crucial to determine whether TMA causes chronic kidney injury.

The death of parenchymal cells and subsequent proliferation of non-adaptive cells contribute to the pathogenesis of kidney disease. In this process, the dysregulation of programmed cell death (PCD) pathways, including apoptosis, ferroptosis, necroptosis, and pyroptosis, plays a crucial role [10]. Several studies have suggested that TMAO aggravates organ damage by activating PCD pathways. For example, TMAO exacerbated cognitive dysfunction and neuropathological changes by increasing oxidative stress-induced neuroinflammation and apoptosis [11]. TMAO also enhanced the infiltration of M1 macrophages in the atria and induced cardiac pyroptosis, ultimately causing atrial structural remodeling [12]. However, whether and which PCD is involved in TMA-induced chronic kidney injury has not been previously evaluated.

Therefore, the present study was aimed to investigate whether TMA contributes to chronic kidney injury and the precise molecular mechanisms involved.

Material and Methods

Animals and treatments

Male C57BL/6J mice purchased from Vital River Laboratories (Beijing, China), were housed in plastic cages with 12 h light/12 h dark cycles at 22-24 °C with 60 % humidity and *ad libitum* access to standard rat chow and sterile tap water.

To observe the effect of TMA, male C57BL/6J mice were randomly divided into two groups (n=8): the Control group and the TMA group. The mice in the TMA group were intraperitoneally injected with TMA (100 μmol/kg/day, Aladdin Biochemical Technology Co., Ltd., China) for three months, whereas the mice in the Control group were injected with normal saline for the same period.

After three months, the mice were euthanized by intraperitoneally injecting an overdose of pentobarbital (100 mg/kg). Subsequently, blood was collected from the abdominal aorta to obtain plasma. The kidney tissue samples were rapidly removed and frozen at -80 °C or fixed with 4 % paraformaldehyde until further analysis.

All animal experiments were performed according to the Guide for the Care and Use of Laboratory Animals published by the US National Institutes of Health (NIH Publication, 8th Edition, 2011) and approved by the Ethics Committee for Laboratory Animals Care and Use of Hebei Medical University.

Measurements of creatinine (Cre) and blood urea nitrogen (BUN) concentrations in plasma

Mouse blood samples were collected in EDTA anticoagulant tubes and immediately centrifuged at 1200× g for 15 min to obtain plasma.

Plasma Cre levels were measured using Cre assay kits (Jiancheng Bioengineering Institute, China). Briefly, after the reagents were added in turn, the samples were incubated at 37 °C for 5 min twice according to the manufacturer's instructions. The absorbance was then measured twice at 546 nm, and the Cre content was calculated using two absorbances according to the formula.

Plasma BUN levels were measured using BUN assay kits (Jiancheng Bioengineering Institute, China). Briefly, reagent preparation and reaction system addition were performed following the manufacturer's instructions. After incubation at 37 °C for 10 min, absorbance was measured at 640 nm.

Masson's trichrome analysis

After being fixed in 4 % paraformaldehyde for 48 h, the kidney tissues were dehydrated, permeabilized, embedded in paraffin, sectioned at 5-μm thickness, and stained with Masson's trichrome to identify collagen deposition, which is shown in blue. Renal sections were examined using an optical microscope (Olympus, Japan) and the collagen volume fraction was calculated as the percentage of collagen (blue-stained area) relative to the total renal area under direct vision.

TUNEL staining

Apoptotic levels in kidney tissue samples were evaluated using a terminal deoxynucleotidyl transferase dUTP nick-end labeling (TUNEL) assay with

a TUNEL apoptosis detection kit (Roche, the United States) following the manufacturer's instructions. Cell nuclei that stained red were defined as TUNEL-positive nuclei and were monitored using a fluorescence microscope (Olympus, Japan).

Measurements of malondialdehyde (MDA) and iron levels in kidney tissue samples

The levels of MDA in the kidney tissue samples were measured using MDA assay kits (Jiancheng Bioengineering Institute, China). After mechanical homogenization and centrifugation, the protein concentration in the supernatant was quantified using the BCA method (Beytime Institute of Biotechnology, China). Subsequently, reagent preparation and reaction system addition were performed following the manufacturer's instructions. After boiling for 40 min and cooling, the absorbance was measured at 532 nm. MDA concentrations were standardized using protein content.

The iron levels in the kidney tissue samples were measured using iron assay kits (Jiancheng Bioengineering Institute, China). After mechanical homogenization and centrifugation, the protein concentration in the supernatant was quantified using the BCA method (Beytime Institute of Biotechnology, China). Subsequently, reagent preparation and reaction system addition were performed following the manufacturer's instructions. Samples were boiled for 5 min, cooled, and centrifuged at 1200× g for 20 min. The absorbance of the supernatants was measured at 520 nm. The iron concentrations were standardized by protein content.

Western blot analysis

Frozen kidney tissue samples were homogenized with ice-cold RIPA lysis buffer. Proteins were extracted and quantified using the BCA method. Equal amounts of protein samples were separated on 10 % SDS-PAGE gels and transferred to polyvinylidene fluoride membranes. The membranes were blocked with 5 % non-fat milk for 1 h and incubated with primary antibodies that recognized Z-DNA binding protein 1 (ZBP1, 1:500, Proteintech Biotechnology, the United States), Caspase-8 (1:500, Proteintech Biotechnology, the United States), NOD-like receptor protein 3 (NLRP3, 1:1000, Proteintech Biotechnology, the United States), Caspase-1 (1:1000, Proteintech Biotechnology, the United States), interleukin-1β (IL-1β, 1:1000, Proteintech Biotechnology, the United States), mixed-lineage kinase domain-like pseudokinase (MLKL, 1:2000, Proteintech Biotechnology, the United States), phosphorylation of MLKL (p-MLKL, 1:1000, Abcam, the United States), receptor-interacting protein kinase 1 (RIP1, 1:1000, Proteintech Biotechnology, the United States), phosphorylation of RIP1 (p-RIP1, 1:1000, Abcam, the United States), receptor-interacting protein kinase 3 (RIP3, 1:1000, Proteintech Biotechnology, the United States), phosphorylation of RIP3 (p-RIP3, 1:1000, Abcam, the United States), Bcl-2-associated X protein (Bax, 1:1000, Proteintech Biotechnology, the United States), B-cell lymphoma-2 (Bcl-2, 1:1000, Proteintech Biotechnology, the United States), nuclear factor erythroid 2-related factor 2 (NRF2, 1:1000, Proteintech Biotechnology, the United States), glutathione peroxidase 4 (GPX4, 1:1000, Proteintech Biotechnology, the United States), ferroportin (FPN, 1:2000, Proteintech Biotechnology, the United States), ferritin heavy chain (FTH, 1:2000, Immunoway, the United States), transferrin receptor 1 (TFR1, 1:1000, Abcam, the United States), and GAPDH (1:5000, Proteintech Biotechnology, the United States) at 4 °C overnight. The membranes were then incubated with horseradish peroxidase-conjugated secondary antibodies for 1 h after washing with TBST. Specific bands were detected using supersignal west Pico chemiluminescent substrate (Thermo, Scientific-Pierce, the United States). The band intensity was quantified using Image J software.

Statistical analysis

Results were presented as mean ± SEM and statistical significance was assessed with SPSS (SPSS 17.0, Inc., the United States) using an independent *t*-test to compare values between two groups. $P<0.05$ was considered statistically significant.

Results

TMA induced chronic kidney injury

As was shown in Figure 1, the plasma Cre (Fig. 1A) and BUN (Fig. 1B) levels, indicators of kidney function, increased significantly in the TMA group as compared with those in the Control group. Additionally, the results of Masson staining assay showed that TMA treatment led to a larger area of fibrosis than the Control group (Fig. 1C-D).

Apoptosis was not involved in TMA-induced chronic kidney injury

As was shown in Figure 2A, TMA treatment did not affect the Bax/Bcl-2 ratio (Fig. 2A). Additionally, no

TUNEL-positive cells (stained with red fluorescence) were found in the kidney tissue samples after TMA treatment (Fig. 2B). These results indicated that apoptosis was not involved in TMA-induced chronic kidney injury.

Ferroptosis was not involved in TMA-induced chronic kidney injury

As was shown in Figure 3, compared with the Control group, TFR1 (Fig. 3A), FTH (Fig. 3B), FPN (Fig. 3C), and NRF2 (Fig. 3E) protein expression in kidney tissue samples was significantly downregulated in the TMA group, whereas GPX4 protein expression was significantly upregulated (Fig. 3F). However, no significant difference in the iron (Fig. 3D) and MDA (Fig. 3G) levels was found between the TMA and Control groups. These results indicated that ferroptosis was not involved in TMA-induced chronic kidney injury.

RIP1/RIP3/MLKL-mediated necroptosis was not involved in TMA-induced chronic kidney injury

As was shown in Figure 4, compared with the Control group, TMA treatment did not change the phosphorylation of RIP1 (Fig. 4A), RIP3 (Fig. 4B), and MLKL (Fig. 4C), indicating that RIP1/RIP3/MLKL-mediated necroptosis was not involved in TMA-induced chronic kidney injury.

NLRP3 inflammasome-mediated pyroptosis was involved in TMA-induced chronic kidney injury

As was shown in Figure 5, compared with the Control group, TMA treatment significantly upregulated NLRP3 (Fig. 5A), Caspase-1 (Fig. 5B), and IL-1β (Fig. 5C) protein expression in the kidney tissue samples, indicating that NLRP3 inflammasome-mediated pyroptosis was involved in TMA-induced chronic kidney injury.

ZBP1 mediated TMA-induced chronic kidney injury

As was shown in Figure 6, compared with the Control group, TMA treatment significantly upregulated cleaved-Caspase 8 (Fig. 6A), Caspase-8 (Fig. 6B), and ZBP1 (Fig. 6C) protein expression in the kidney tissue samples. These results indicated that ZBP1-mediated cell death was involved in TMA-induced chronic kidney injury.

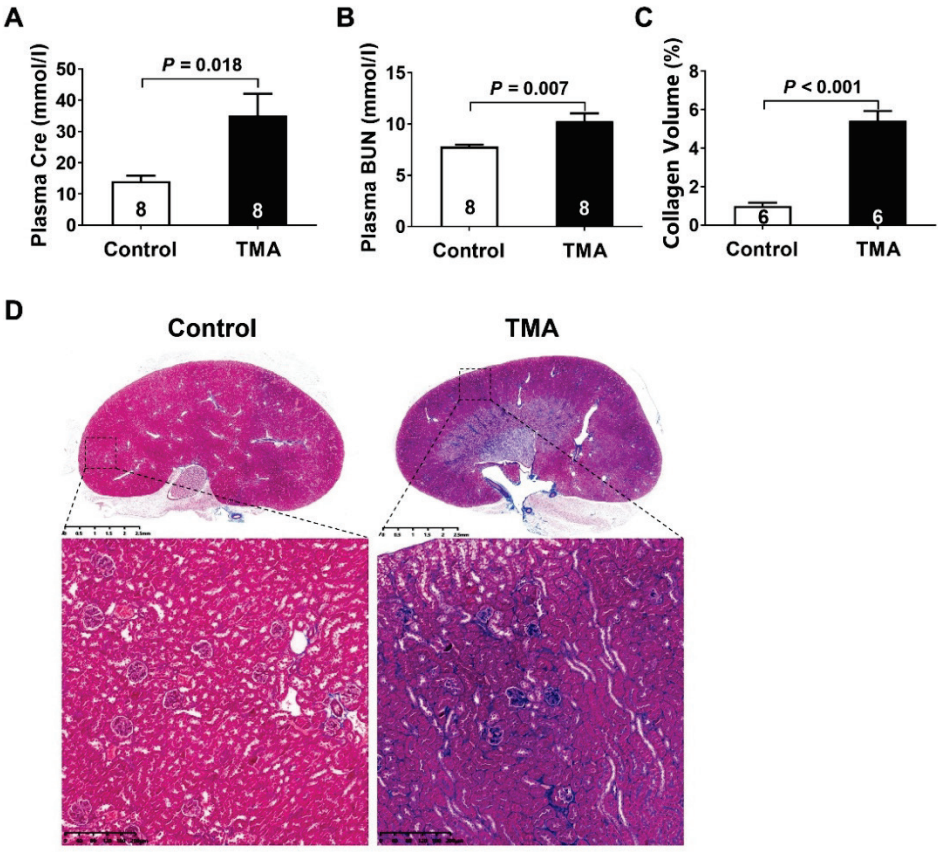

Fig. 1. TMA induced chronic kidney injury. (**A**) Creatinine (Cre) levels in the plasma after TMA treatment. (**B**) Blood urea nitrogen (BUN) levels in the plasma after TMA treatment. (**C**) The quantitative analysis for collagen volume fraction (%) in kidney tissues after TMA treatment. (**D**) Representative Masson's trichrome-stained kidney sections after TMA treatment. Results are expressed as mean ± SEM. A $P<0.05$ was considered significant.

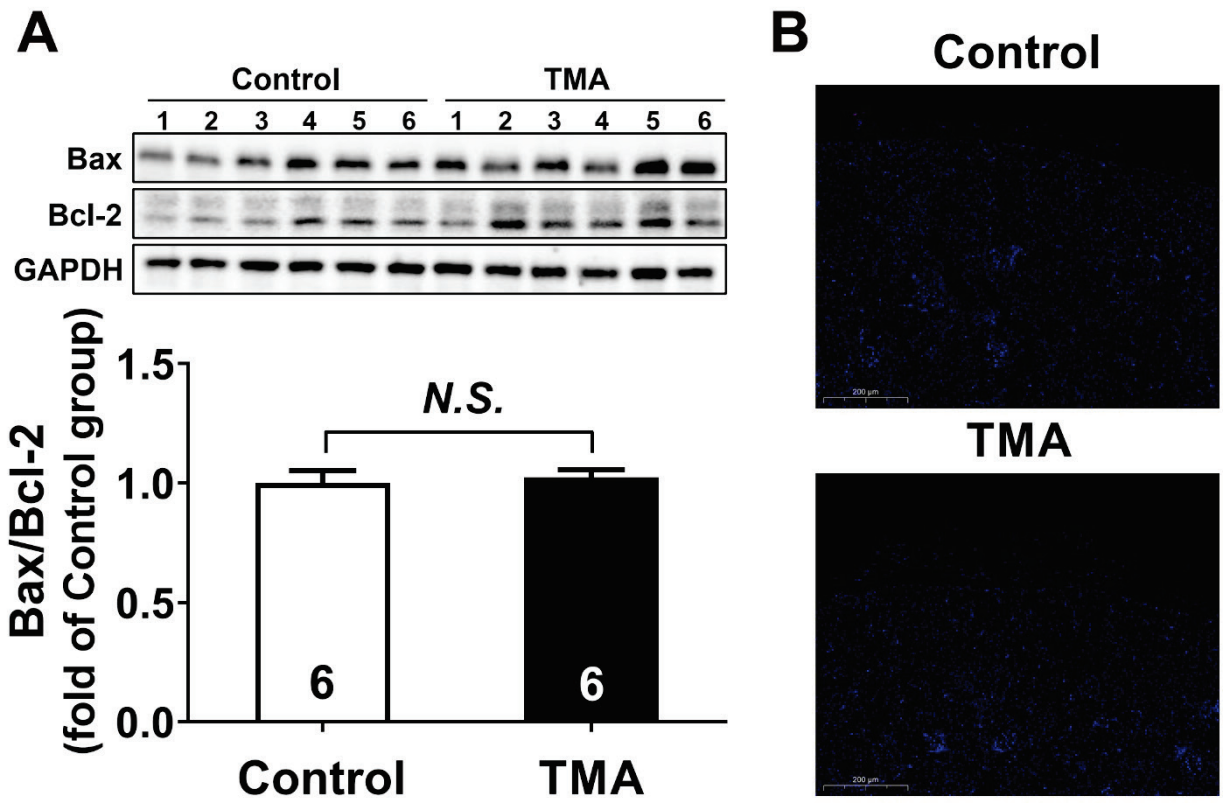

Fig. 2. Apoptosis was not involved in TMA-induced chronic kidney injury. (**A**) Representative Western blots and quantitative analysis for Bax/Bcl-2 protein expression in kidney tissues after TMA treatment. (**B**) Representative TUNEL-stained kidney sections after TMA treatment. Results are expressed as mean ± SEM. A P<0.05 was considered significant.

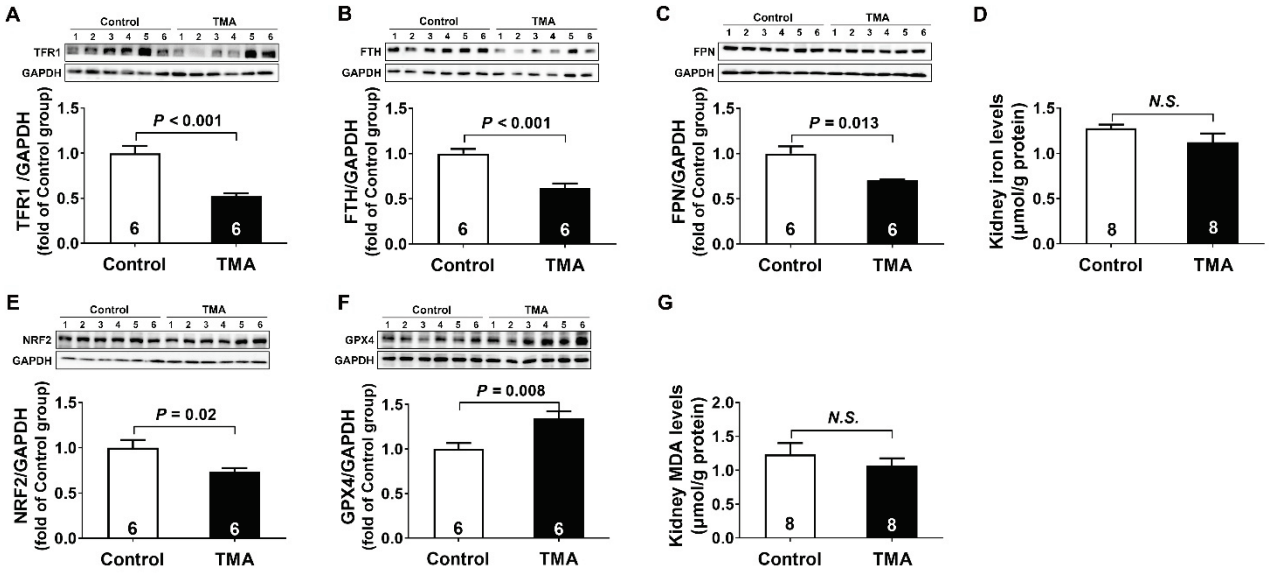

Fig. 3. Ferroptosis was not involved in TMA-induced chronic kidney injury. (**A-C**) Representative Western blots and quantitative analysis for TFR1, FTH, and FPN protein expression in kidney tissues after TMA treatment. (**D**) Iron levels in kidney tissues after TMA treatment. (**E-F**) Representative Western blots and quantitative analysis for NRF2 and GPX4 protein expression in kidney tissues after TMA treatment. (**G**) MDA levels in kidney tissues after TMA treatment. Results are expressed as mean ± SEM. A P<0.05 was considered significant.

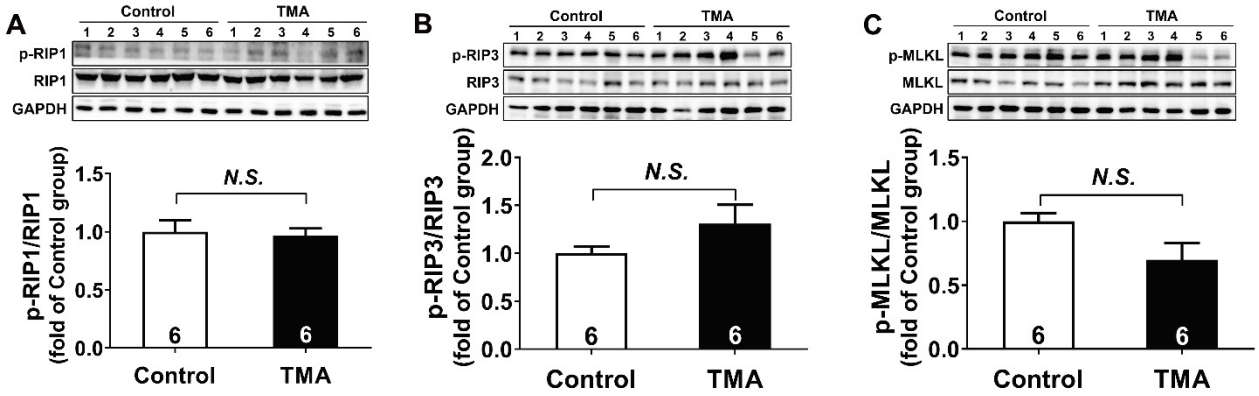

Fig. 4. RIP1/RIP3/MLKL-mediated necroptosis was not involved in TMA-induced chronic kidney injury. (**A-C**) Representative Western blots and quantitative analysis for p-RIP1/RIP1, p-RIP3/RIP3 and p-MLKL/MLKL protein expression in kidney tissues after TMA treatment. Results are expressed as mean ± SEM. A P<0.05 was considered significant.

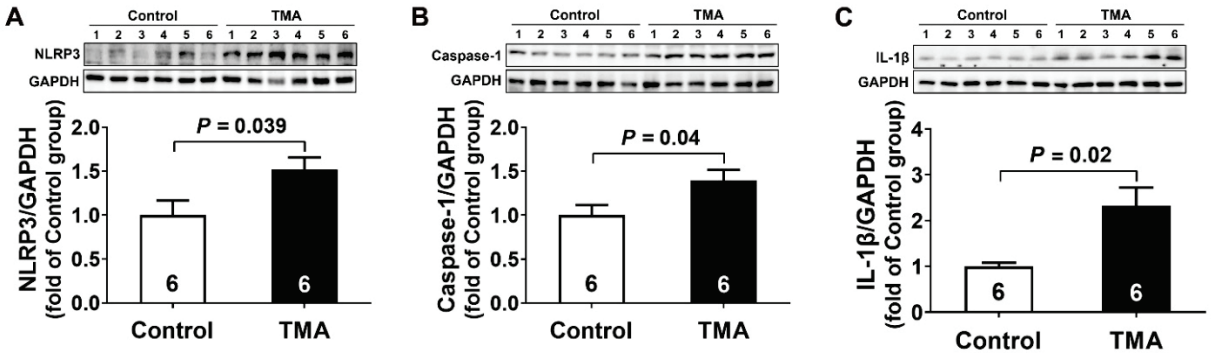

Fig. 5. NLRP3 inflammasome-mediated pyroptosis was involved in TMA-induced chronic kidney injury. (**A-C**) Representative Western blots and quantitative analysis for NLRP3, Caspase-1, and IL-1β protein expression in kidney tissues after TMA treatment. Results are expressed as mean ± SEM. A P<0.05 was considered significant.

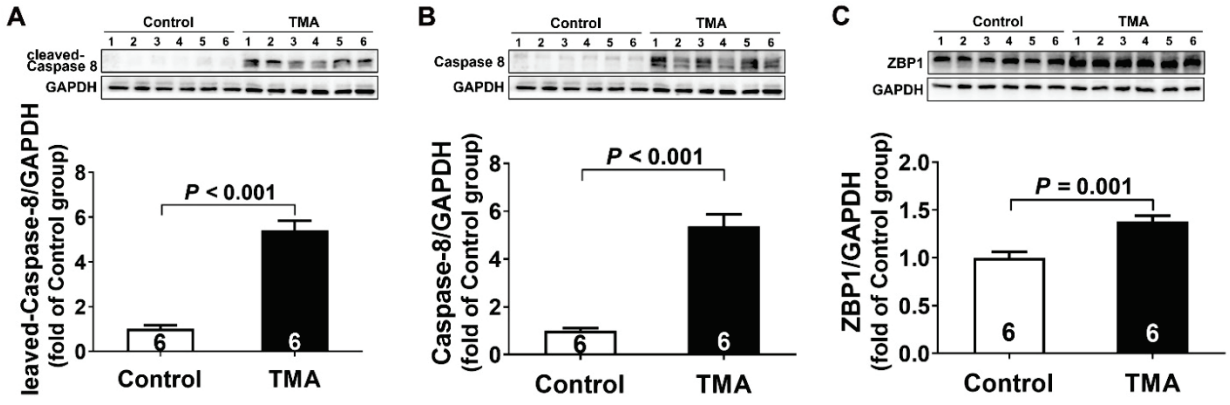

Fig. 6. ZBP1 mediated TMA-induced chronic kidney injury. (**A-C**) Representative Western blots and quantitative analysis for cleaved-Caspase 8, Caspase-8, and ZBP1 protein expression in kidney tissues after TMA treatment. Results are expressed as mean ± SEM. A P<0.05 was considered significant.

Discussion

The results of this study demonstrated that TMA directly damaged the kidney and that the ZBP1-NLRP3 inflammasome pathway was involved in TMA-induced chronic kidney injury.

TMAO is a gut-microbiota metabolite derived from diets rich in choline, phosphatidylcholine, betaine, and carnitine. Given that the kidney mostly clears plasma TMAO, elevated TMAO concentration associates positively with renal impairment and dysfunction. Furthermore, TMAO directly caused progressive renal

fibrosis and dysfunction in animal models [7]. The present study showed that plasma Cre and BUN levels, indicators of kidney function, increased significantly in mice treated with TMA. The Masson staining assay showed that TMA treatment led to a larger fibrosis area than the Control group. These results suggested that TMA could directly cause kidney injury and fibrosis. In line with our findings, inhibition of TMA generation using a choline TMA-lyase inhibitor, which effectively blocked the conversion of choline into TMA, attenuated CKD development and preserved kidney function [13]. According to the literature, PCD pathways, including apoptosis, ferroptosis, necroptosis, and pyroptosis, play a crucial role in the pathogenesis of kidney diseases, including CKD [14]. However, whether PCD is involved in TMA-induced chronic kidney injury and its exact molecular mechanisms remain unclear.

As a classic form of cell death, apoptosis plays a well-established role in the pathophysiology of kidney diseases [15]. It was reported that TMAO could promote hyperoxaluria-induced kidney injury by activating apoptosis [16]. Yong *et al.* also reported that TMAO induced renal tubule apoptosis by regulating ASK1-JNK phosphorylation [17]. However, in the present study, no apoptosis was found in kidney tissue samples after direct treatment with TMA, indicating that TMA-induced chronic kidney injury was not caused by oxidation to TMAO *in vivo*.

Ferroptosis is a newly recognized type of PCD that differs morphologically, biochemically, and genetically from other types of PCD. Iron overload, which originates from abnormal iron metabolism or maladjustment of redox systems, is the key trigger of ferroptosis [18-19]. Cellular iron homeostasis is tightly regulated by a dynamic process that includes iron uptake, storage, and export. Iron uptake relies primarily on TFR1, which internalizes transferrin-bound iron. Cytoplasmic iron is stored in ferritin, an iron storage protein complex comprising ferritin light chain and FTH. Furthermore, excess Fe^{2+} can be oxidized to Fe^{3+} and exported by FPN. Under pathological conditions, excessive iron induces the rapid accumulation of intracellularly lethal reactive oxygen species (ROS) through the Fenton reaction. If the activity of antioxidant systems, including GPX4 and NRF2 decreases, ROS will not be scavenged in time, contributing to subsequent lipid peroxidation and triggering ferroptosis. Recently, ferroptosis has been studied primarily in acute kidney injury (AKI), but studies on ferroptosis and CKD remain limited [20]. In the present study, treatment with TMA for three months caused chronic kidney injury, and TFR1, FTH, FPN, and NRF2 protein expression in kidney tissue samples was significantly downregulated, whereas GPX4 protein expression was significantly upregulated. However, compared with the Control group, TMA treatment induced insignificant changes in iron and MDA contents, which are key molecular markers for detecting of ferroptosis and lipid peroxidation. These results indicated that ferroptosis was not involved in TMA-induced chronic kidney injury, and that changes in TFR1, FTH, FPN, NRF2, and GPX4 protein expression may be caused by a compensatory mechanism. Ferroptosis could have occurred during AKI, however, in the process of AKI transforming into CKD, ferroptosis markers tended to remain at normal levels through compensation. Consistent with this study, no increase in iron content was found even in cells developing ferroptosis or kidney tissues of mice with AKI [21]. Another study also found that tocilizumab mimotope alleviated renal fibrosis by regulating the ferroptosis signaling pathway, but they failed to directly prove that ferroptosis was involved in this progression [22]. Considering that studies involving TMA or TMAO-induced CKD and ferroptosis remain lacking, a better understanding of the relevant mechanisms needed to be further carried out.

Apoptosis or ferroptosis was reportedly more involved in AKI [23]. Pyroptosis and necroptosis, the lytic, inflammatory types of PCD, were found to play important roles in the progression of AKI into CKD and result in lasting tissue injury [24-25].

Necroptosis is an inflammatory form of cell death that can be triggered by perturbations in extracellular or intracellular homeostasis through death receptors, toll-like receptors, or cytoplastic nucleic acid sensor ZBP1. Activation of these receptors leads to necrosome assembly which consists of RIP1, RIP3 and its substrate MLKL. Subsequent RIP3-mediated phosphorylation of MLKL triggers MLKL oligomerization and translocation to the plasma membrane to disrupt membrane integrity and cause cytokine and potassium efflux, leading to inflammation responses termed necroinflammation [26-27]. RIP3, MLKL, and p-MLKL were upregulated in patients with CKD, suggesting that necroptosis of renal tubular epithelial cells occurred, which mediated renal tubular interstitial fibrosis [28]. Contrarily, RIP3 and MLKL deficiency or knockdown prevented the tubular interstitial fibrosis [29]. In the present study, we found that treatment with TMA

did not change RIP1, RIP3 and MLKL phosphorylation, indicating that RIP1/RIP3/MLKL-mediated necroptosis was not involved in TMA-induced chronic kidney injury. Furthermore, whether TMAO induces kidney injury through necroptosis remains unreported.

Pyroptosis is another inflammatory form of cell death triggered by certain inflammasomes leading to cell swelling, membrane perforation, and the release of intracellular contents. The NLRP3 inflammasome, a multimolecular complex including NLRP3 (a sensor protein), an apoptosis-associated speck-like protein containing CARD (an adapter protein), and procaspase-1 (an effector protease), is a core player in the canonical pathway of pyroptosis. After recognizing endogenous and exogenous stimuli, the expression of the NLRP3 inflammasome protein is upregulated, and then assembled and activated. Once activated, it excites caspase-1, leading to the IL-1β and IL-18 maturation and secretion [30-31]. Several studies have suggested that pyroptosis contributes to the transition from AKI to CKD and the development of kidney fibrosis directly or by stimulating inflammatory responses [32]. In this study, TMA treatment significantly upregulated NLRP3, Caspase-1, and IL-1β protein expression in kidney tissue samples, indicating that NLRP3 inflammasome-mediated pyroptosis was involved in TMA-induced chronic kidney injury. Currently, no research on TMA directly leading to pyroptosis exists. However, TMAO has been found to be involved in various diseases by inducing pyroptosis. It was revealed that TMAO-induced graft-versus-host disease progression was mediated by polarized M1 macrophages requiring NLRP3 inflammasome activation [33]. In addition, TMAO promoted vascular calcification by activating of NLRP3 inflammasome signals [34]. The inhibition of TMAO attenuated neointimal formation by reducing the inflammasome in a mouse model of carotid artery ligation [35].

ZBP1 was initially recognized as a key cytoplasmic sensor for viral and endogenous nucleic acid ligands that trigger innate immune responses. Recent studies have highlighted its central role in the inflammatory PCD pathway by forming the ZBP1-RIP3-FADD-cassase-8 complex, a large multifaceted cell death complex called the ZBP1-PANoptosome. Upon activation, ZBP1 initiates ZBP1-PANoptosome assembly to drive pyroptosis and necroptosis, causing cell death and inflammation [36-37]. In this study, TMA treatment significantly upregulated cleaved-Caspase 8, Caspase-8, and ZBP1 protein expression in kidney tissue samples. Meanwhile, although the necroptosis pathway protein changed insignificantly, the pyroptosis pathway protein was significantly upregulated. These results indicated that the ZBP1-NLRP3 inflammasome pathway was involved in TMA-induced chronic kidney injury. Consistent with our findings, it has been reported that ZBP1 regulated NLRP3 inflammasome activation and proinflammatory cytokine production during IAV infection independent of the necroptosis executioner MLKL [38]. ZBP1 was also found to promote hepatocellular pyroptosis [39], whereas inhibition of ZBP1/NLRP3 pathway-mediated pyroptosis could attenuate acute pancreatitis [40].

This study had several limitations. First, TMA could be converted into TMAO, which was closely related to CKD, by hepatic flavin monooxygenases, therefore, the role of TMAO in TMA-induced chronic kidney injury could not be ruled out and should be considered. Second, we evaluated whether apoptosis, ferroptosis, necroptosis, and pyroptosis were involved in TMA-induced chronic kidney injury and found that TMA induced chronic kidney injury *via* ZBP1-NLRP3 inflammasome pathway-mediated pyroptosis. However, other forms of PCD, such as autophagy should be considered.

In conclusion, our studies revealed that the ZBP1-NLRP3 inflammasome may take part in the progression of TMA induced chronic kidney injury.

Conflict of Interest

There is no conflict of interest.

Acknowledgements

This study was supported by the National Natural Science Foundation of China (32271155, 91849120, and 31871154).

References

1. Ruiz-Ortega M, Rayego-Mateos S, Lamas S, Ortiz A, Rodrigues-Diez RR. Targeting the progression of chronic kidney disease. Nat Rev Nephrol 2020;16:269-288. https://doi.org/10.1038/s41581-019-0248-y
2. Wang H, Ainiwaer A, Song Y, Qin L, Peng A, Bao H, Qin H. Perturbed gut microbiome and fecal and serum metabolomes are associated with chronic kidney disease severity. Microbiome 2023;11:3. https://doi.org/10.1186/s40168-022-01443-4

3. Janeiro MH, Ramírez MJ, Milagro FI, Martínez JA, Solas M. Implication of Trimethylamine N-Oxide (TMAO) in Disease: Potential Biomarker or New Therapeutic Target. Nutrients 2018;10:1398. https://doi.org/10.3390/nu10101398
4. Zixin Y, Lulu C, Xiangchang Z, Qing F, Binjie Z, Chunyang L, Tai R, Dongsheng O. TMAO as a potential biomarker and therapeutic target for chronic kidney disease: A review. Front Pharmacol 2022;13:929262. https://doi.org/10.3389/fphar.2022.929262
5. Stubbs JR, House JA, Ocque AJ, Zhang S, Johnson C, Kimber C, Schmidt K, ET AL. Serum Trimethylamine-N-Oxide is Elevated in CKD and Correlates with Coronary Atherosclerosis Burden. J Am Soc Nephrol 2016;27:305-313. https://doi.org/10.1681/ASN.2014111063
6. Gupta N, Buffa JA, Roberts AB, Sangwan N, Skye SM, Li L, Ho KJ, ET AL. Targeted Inhibition of Gut Microbial Trimethylamine N-Oxide Production Reduces Renal Tubulointerstitial Fibrosis and Functional Impairment in a Murine Model of Chronic Kidney Disease. Arterioscler Thromb Vasc Biol 2020;40:1239-1255. https://doi.org/10.1161/ATVBAHA.120.314139
7. Tang WH, Wang Z, Kennedy DJ, Wu Y, Buffa JA, Agatisa-Boyle B, Li XS, Levison BS, Hazen SL. Gut microbiota-dependent trimethylamine N-oxide (TMAO) pathway contributes to both development of renal insufficiency and mortality risk in chronic kidney disease. Circ Res 2015;116:448-455. https://doi.org/10.1161/CIRCRESAHA.116.305360
8. Gawrys-Kopczynska M, Konop M, Maksymiuk K, Kraszewska K, Derzsi L, Sozanski K, Holyst R, ET AL. TMAO, a seafood-derived molecule, produces diuresis and reduces mortality in heart failure rats. Elife 2020;9:e57028. https://doi.org/10.7554/eLife.57028
9. Jaworska K, Hering D, Mosieniak G, Bielak-Zmijewska A, Pilz M, Konwerski M, Gasecka A, ET AL. TMA, A Forgotten Uremic Toxin, but Not TMAO, Is Involved in Cardiovascular Pathology. Toxins (Basel) 2019;11:490. https://doi.org/10.3390/toxins11090490
10. Guerrero-Mauvecin J, Villar-Gómez N, Rayego-Mateos S, Ramos AM, Ruiz-Ortega M, Ortiz A, Sanz AB. Regulated necrosis role in inflammation and repair in acute kidney injury. Front Immunol 2023;14:1324996. https://doi.org/10.3389/fimmu.2023.1324996
11. Deng Y, Zou J, Hong Y, Peng Q, Fu X, Duan R, Chen J, Chen X. Higher Circulating Trimethylamine N-Oxide Aggravates Cognitive Impairment Probably via Downregulating Hippocampal SIRT1 in Vascular Dementia Rats. Cells 2022;11:3650. https://doi.org/10.3390/cells11223650
12. Luo Y, Zhang Y, Han X, Yuan Y, Zhou Y, Gao Y, Yu H, ET AL. Akkermansia muciniphila prevents cold-related atrial fibrillation in rats by modulation of TMAO induced cardiac pyroptosis. EBioMedicine 2022;82:104087. https://doi.org/10.1016/j.ebiom.2022.104087
13. Zhang W, Miikeda A, Zuckerman J, Jia X, Charugundla S, Zhou Z, Kaczor-Urbanowicz KE, ET AL. Inhibition of microbiota-dependent TMAO production attenuates chronic kidney disease in mice. Sci Rep 2021;11:518. https://doi.org/10.1038/s41598-020-80063-0
14. Sanz AB, Sanchez-Niño MD, Ramos AM, Ortiz A. Regulated cell death pathways in kidney disease. Nat Rev Nephrol 2023;19:281-299. https://doi.org/10.1038/s41581-023-00694-0
15. Sanz AB, Santamaría B, Ruiz-Ortega M, Egido J, Ortiz A. Mechanisms of renal apoptosis in health and disease. J Am Soc Nephrol 2008;19:1634-1642. https://doi.org/10.1681/ASN.2007121336
16. Dong F, Jiang S, Tang C, Wang X, Ren X, Wei Q, Tian J, ET AL. Trimethylamine N-oxide promotes hyperoxaluria-induced calcium oxalate deposition and kidney injury by activating autophagy. Free Radic Biol Med 2022;179:288-300. https://doi.org/10.1016/j.freeradbiomed.2021.11.010
17. Yong C, Huang G, Ge H, Zhu Y, Yang Y, Yu Y, Tian F, ET AL. Perilla frutescens L. alleviates trimethylamine N-oxide-induced apoptosis in the renal tubule by regulating ASK1-JNK phosphorylation. Phytother Res 2023;37:1274-1292. https://doi.org/10.1002/ptr.7684
18. Jiang X, Stockwell BR, Conrad M. Ferroptosis: mechanisms, biology and role in disease. Nat Rev Mol Cell Biol 2021;22:266-282. https://doi.org/10.1038/s41580-020-00324-8
19. Sun S, Shen J, Jiang J, Wang F, Min J. Targeting ferroptosis opens new avenues for the development of novel therapeutics. Signal Transduct Target Ther 2023;8:372. https://doi.org/10.1038/s41392-023-01606-1

20. Wang J, Liu Y, Wang Y, Sun L. The Cross-Link between Ferroptosis and Kidney Diseases. Oxid Med Cell Longev 2021;2021:6654887. https://doi.org/10.1155/2021/6654887
21. Wang Y, Quan F, Cao Q, Lin Y, Yue C, Bi R, Cui X, ET AL. Quercetin alleviates acute kidney injury by inhibiting ferroptosis. J Adv Res 2020;28:231-243. https://doi.org/10.1016/j.jare.2020.07.007
22. Yang L, Guo J, Yu N, Liu Y, Song H, Niu J, Gu Y. Tocilizumab mimotope alleviates kidney injury and fibrosis by inhibiting IL-6 signaling and ferroptosis in UUO model. Life Sci 2020;261:118487. https://doi.org/10.1016/j.lfs.2020.118487
23. Maremonti F, Meyer C, Linkermann A. Mechanisms and Models of Kidney Tubular Necrosis and Nephron Loss. J Am Soc Nephrol 2022;33:472-486. https://doi.org/10.1681/ASN.2021101293
24. Chen H, Fang Y, Wu J, Chen H, Zou Z, Zhang X, Shao J, Xu Y. RIPK3-MLKL-mediated necroinflammation contributes to AKI progression to CKD. Cell Death Dis 2018;9:878. https://doi.org/10.1038/s41419-018-0936-8
25. Chen Z, Chen C, Lai K, Wu C, Wu F, Chen Z, Ye K, ET AL. GSDMD and GSDME synergy in the transition of acute kidney injury to chronic kidney disease. Nephrol Dial Transplant 2024;39:1344-1359. https://doi.org/10.1093/ndt/gfae014
26. Pasparakis M, Vandenabeele P. Necroptosis and its role in inflammation. Nature 2015;517:311-320. https://doi.org/10.1038/nature14191
27. Galluzzi L, Kepp O, Chan FK, Kroemer G. Necroptosis: Mechanisms and Relevance to Disease. Annu Rev Pathol 2017;12:103-130. https://doi.org/10.1146/annurev-pathol-052016-100247
28. Lin Z, Chen A, Cui H, Shang R, Su T, Li X, Wang K, ET AL. Renal tubular epithelial cell necroptosis promotes tubulointerstitial fibrosis in patients with chronic kidney disease. FASEB J 2022;36:e22625. https://doi.org/10.1096/fj.202200706RR
29. Srivastava A, Tomar B, Sharma P, Kumari S, Prakash S, Rath SK, Kulkarni OP, ET AL. RIPK3-MLKL signaling activates mitochondrial CaMKII and drives intrarenal extracellular matrix production during CKD. Matrix Biol 2022;112:72-89. https://doi.org/10.1016/j.matbio.2022.08.005
30. Yu P, Zhang X, Liu N, Tang L, Peng C, Chen X. Pyroptosis: mechanisms and diseases. Signal Transduct Target Ther 2021;6:128. https://doi.org/10.1038/s41392-021-00507-5
31. Elias EE, Lyons B, Muruve DA. Gasdermins and pyroptosis in the kidney. Nat Rev Nephrol 2023;19:337-350. https://doi.org/10.1038/s41581-022-00662-0
32. Liu Y, Lei H, Zhang W, Xing Q, Liu R, Wu S, Liu Z, ET AL. Pyroptosis in renal inflammation and fibrosis: current knowledge and clinical significance. Cell Death Dis 2023;14:472. https://doi.org/10.1038/s41419-023-06005-6
33. Wu K, Yuan Y, Yu H, Dai X, Wang S, Sun Z, Wang F, ET AL. The gut microbial metabolite trimethylamine N-oxide aggravates GVHD by inducing M1 macrophage polarization in mice. Blood 2020;136:501-515. https://doi.org/10.1182/blood.2019003990
34. Zhang X, Li Y, Yang P, Liu X, Lu L, Chen Y, Zhong X, ET AL. Trimethylamine-N-Oxide Promotes Vascular Calcification Through Activation of NLRP3 (Nucleotide-Binding Domain, Leucine-Rich-Containing Family, Pyrin Domain-Containing-3) Inflammasome and NF-κB (Nuclear Factor κB) Signals. Arterioscler Thromb Vasc Biol 2020;40:751-765. https://doi.org/10.1161/ATVBAHA.119.313414
35. Chen CY, Leu HB, Wang SC, Tsai SH, Chou RH, Lu YW, Tsai YL, ET AL. Inhibition of Trimethylamine N-Oxide Attenuates Neointimal Formation Through Reduction of Inflammasome and Oxidative Stress in a Mouse Model of Carotid Artery Ligation. Antioxid Redox Signal 2023;38:215-233. https://doi.org/10.1089/ars.2021.0115
36. Lee S, Karki R, Wang Y, Nguyen LN, Kalathur RC, Kanneganti TD. AIM2 forms a complex with pyrin and ZBP1 to drive PANoptosis and host defence. Nature 2021;597:415-419. https://doi.org/10.1038/s41586-021-03875-8
37. Banoth B, Tuladhar S, Karki R, Sharma BR, Briard B, Kesavardhana S, Burton A, Kanneganti TD. ZBP1 promotes fungi-induced inflammasome activation and pyroptosis, apoptosis, and necroptosis (PANoptosis). J Biol Chem 2020;295:18276-18283. https://doi.org/10.1074/jbc.RA120.015924
38. Malireddi RKS, Sharma BR, Bynigeri RR, Wang Y, Lu J, Kanneganti TD. ZBP1 Drives IAV-Induced NLRP3 Inflammasome Activation and Lytic Cell Death, PANoptosis, Independent of the Necroptosis Executioner MLKL. Viruses 2023;15:2141. https://doi.org/10.3390/v15112141

39. Yan S, Yu L, Chen Z, Xie D, Huang Z, Ouyang S. ZBP1 promotes hepatocyte pyroptosis in acute liver injury by regulating the PGAM5/ROS pathway. Ann Hepatol 2024;29:101475. https://doi.org/10.1016/j.aohep.2024.101475
40. Sun B, Chen Z, Chi Q, Zhang Y, Gao B. Endogenous tRNA-derived small RNA (tRF3-Thr-AGT) inhibits ZBP1/NLRP3 pathway-mediated cell pyroptosis to attenuate acute pancreatitis (AP). J Cell Mol Med 2021;25:10441-10453. https://doi.org/10.1111/jcmm.16972